Analyst

COMMUNICATION

View Article Online
View Journal | View Issue

Cite this: *Analyst*, 2015, **140**, 4981

Received 1st March 2015,
Accepted 19th May 2015

DOI: 10.1039/c5an00392j

www.rsc.org/analyst

Composite SERS-based satellites navigated by optical tweezers for single cell analysis†

Inna Y. Stetciura,[a,b] Alexey Yashchenok,[a,c] Admir Masic,[c] Evgeny V. Lyubin,[d] Olga A. Inozemtseva,[a] Maria G. Drozdova,[e] Elena A. Markvichova,[e] Boris N. Khlebtsov,[f] Andrey A. Fedyanin,[d] Gleb B. Sukhorukov,[g] Dmitry A. Gorin*[a] and Dmitry Volodkin*[b]

Herein, we have designed composite SERS-active micro-satellites, which exhibit a dual role: (i) effective probes for determining cellular composition and (ii) optically movable and easily detectable markers. The satellites were synthesized by the layer-by-layer assisted decoration of silica microparticles with metal (gold or silver) nanoparticles and astralen in order to ensure satellite SERS-based microenvironment probing and satellite recognition, respectively. A combination of optical tweezers and Raman spectroscopy can be used to navigate the satellites to a certain cellular compartment and probe the intracellular composition following cellular uptake. In the future, this developed approach may serve as a tool for single cell analysis with nanometer precision due to the multilayer surface design, focusing on both extracellular and intracellular studies.

Nowadays, single cell analysis is a rapidly developing and highly promising scientific field aiming at the analysis of extracellular and intracellular composition at the single cell level.[1] High heterogeneity of biological cells has stimulated the research towards the biological analysis of a single cell.[2,3] Single cell analysis is quickly being developed in applied fields such as diagnostics and biosensors. A number of different techniques applicable to single cell analysis are rapidly growing, including microfluidics, which gives the option of separating biological cells and reducing analysis volumes.[4,5]

SERS is a non-contact and label-free method already in application and has the strong potential to reveal the composition of biological tissues in real-time.[6,7] This method has high sensitivity, allowing us to detect a single molecule,[8] and approach the challenge of single cell analysis.[9] To date, progress in SERS is limited by the development of new nanostructured materials, which can be used as SERS platforms for biomedical applications. The generation of effective surface enhancements of Raman scattering was demonstrated by specially prepared metal surfaces with high roughness. Various types of rough metal surfaces were obtained by the patterning[10–12] or multistage transfer printing[13] of nanoparticle assemblies made from gold nanorods,[14,15] nanostars,[16,17] mesoflowers,[18] silver nanorods,[19] nanowires[20] and core–shell nanoparticles.[10] Thanks to the great progress in the field of metal nanoparticles synthesis, one of the simplest and most cost-effective strategies to manufacture SERS platforms is to fabricate self-assembled nanoparticles. However, the limitations to using the nanoparticles are caused by their small sizes, leading to great difficulties in their manipulation and detection. More importantly, the acquisition of SERS signals from a single nanoparticle still remains challenging.

In contrast, micrometer sized particles can be easily observed using an optical microscope. Moreover, it is also reported that the microparticles of spherical shape can be easily moved with optical tweezers.[21–23] The layer-by-layer assembly method has already been applied to the formation of nanocomposite shells using SERS platforms.[24,25] The shells can be engulfed by a living cell, allowing SERS-based intracellular analysis.[26] However, as far as we know, there are no studies demonstrating the externally triggered positioning of SERS-active platforms for localized cellular studies. Herein, for the first time, we demonstrate that optical tweezers can be used to position SERS-active microspheres onto a surface of L929 mouse fibroblasts, and the intracellular composition can be probed for the engulfed microspheres.

First, we synthesized composite microparticles to be used as SERS-active satellites. As a solid support, we chose silica microparticles because the particles are well suited for surface modification. The LbL assembly technique allows us to modify the surface of various solid particles to possess certain

[a]*Saratov State University, 410012 Saratov, Russia. E-mail: gorinda@mail.ru*
[b]*Fraunhofer Institute for Cell Therapy and Immunology, Branch Bioanalytics and Bioprocesses (Fraunhofer IZI-BB), 14476 Potsdam-Golm, Germany. E-mail: dmitry.volodkin@izi-bb.fraunhofer.de*
[c]*Max Planck Institute of Colloids and Interfaces Potsdam-Golm, Germany*
[d]*Lomonosov Moscow State University, Faculty of Physics, 119991 Moscow, Russia*
[e]*Shemyakin-Ovchinnikov Institute of Bioorganic Chemistry, RAS, 117997 Moscow, Russia*
[f]*Institute of Biochemistry and Physiology of Plants and Microorganisms RAS, 410049 Saratov, Russia*
[g]*Queen Mary University of London, London, E1 4NS, UK*
†Electronic supplementary information (ESI) available. See DOI: 10.1039/c5an00392j

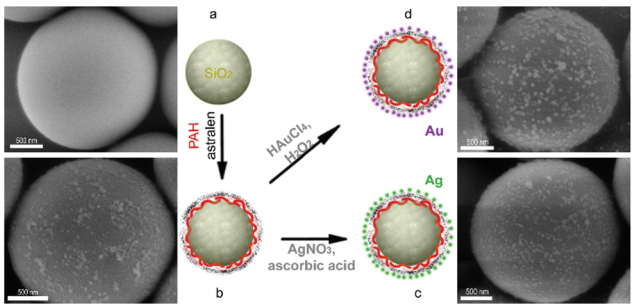

Fig. 1 The scheme of fabrication of SERS-active satellites and corresponding SEM images at every fabrication step: (a) SiO_2 microspheres, (b) SiO_2/(PAH/Astralen)$_3$, (c) SiO_2/(PAH/Astralen)$_3$/Ag and (d) SiO_2/(PAH/Astralen)$_3$/Au microspheres.

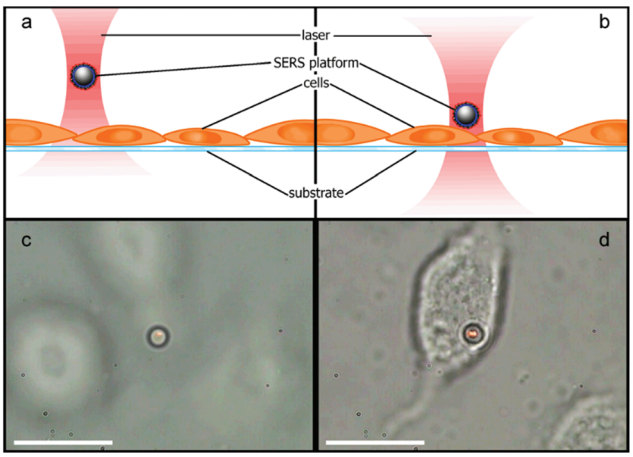

Fig. 2 Schematics of SERS-active satellite transport by laser tweezers to the surface of a cell (a, b). Optical transmission images of a SERS-active satellite trapped by tweezers above a L929 mouse fibroblast cell (c) and in the vicinity of cell membrane (d). For movie see the ESI.† Scale bars in the optical images are 10 μm.

functionality.[27–29] We utilized this approach for making the satellites detectable by Raman spectroscopy. For this purpose, a thin multilayer film ((poly(allylamine hydrochloride)/astralen)$_3$ or (PAH/Astralen)$_3$) was deposited onto the surface of solid silica microparticles (Fig. 1). Astralen serves as a marker that is easily detectable by Raman spectroscopy.[30] PAH is used as a type of "glue molecule", enabling the complexation of astralen particles by the LbL manner to attach astralen onto the microparticle surface. Three bilayers were chosen to ensure enough astralen molecules per particle surface are present.

In the next step, the particles were modified by metal nanoparticles in order to create a surface for the effective enhancement of a Raman signal (Fig. 1). Both gold and silver nanoparticles, as well as films made from these nanoparticles, are known to be effective SERS coatings.[26,31] Gold or silver was chemically reduced to the surface by previously established protocols.[32] The composition of the core–shell microparticles was as follows: silica microparticles/(PAH/astralen)$_3$/Au(or Ag).

SEM analysis clearly demonstrates an increase of the surface roughness after the deposition of the (PAH/astralen)$_3$ film as well as after metal nanoparticle adsorption and subsequent chemical reduction. The surface roughness of the microparticles after the deposition of metal nanoparticles (Au or Ag) is in a comparable size range with the sizes of probed molecules. This increases the chance to get strong enhancement of the Raman signal for biomolecules located in the vicinity of the inhomogeneous metal surface. As shown in our previous study, the deposition of (PAH/astralen)$_3$/Ag onto $CaCO_3$ microparticles leads to an effective enhancement of Raman signals of biomolecules (*e.g.* polylactide and hyaluronic acid) commonly used for tissue engineering applications.[32] However, in contrast to the silver particles, the plasmon peak of the particles coated with gold are red-shifted. This allows the use of infrared laser to carry out the non-invasive manipulation of particles in a living tissue. Therefore, as will be shown later, we tested the SERS activity of the satellites synthesized here in cellular experiments.

As the next step, we tested the capability of holding engineered microparticles by optical tweezers. The holding and subsequent moving were carried out by a continuous-wave diode infrared laser. Both types of satellites (coated with silver or gold nanoparticles) were trapped by a focused laser beam. However, the trapping of the gold-coated satellites was more effective because silver coated particles escaped from the laser trap more often. We believe that this behavior results from the low chemical stability of the silver coatings as compared with gold.[33] Thus, the gold-coated silica-based platform was more effective in providing stable capture by laser tweezers as schematically shown in Fig. 2a and b (see also the video file in the ESI†). According to this scheme, the movement of the laser beam towards the glass substrate results in the simultaneous moving of the captured satellites in the same direction. In the real cellular experiment, the described movement leads to a clear visual observation of the cell (Fig. 2c and d).

The cell is better focused when the satellite approaches the cellular surface. Upon contact of the satellite with the cellular surface, the focused laser was turned off, leading to sticking of the satellite to the cell surface. Thus, one can easily choose a position of interest on the cell surface with micrometer precision and navigate the satellite to this position and subsequently release the satellite. The experiments with cells were carried out both in a PBS buffer and in a culture medium. In both cases, the SERS platforms were successfully taken and consistently held by the laser trap (see video in the ESI†). This demonstrates that the navigation by optical tweezers can be performed under physiological conditions in real cellular experiments.

It is of interest to explore an intracellular environment by the satellites placed in contact with a certain cellular compartment. We found that after contact with the cell surface, the satellites were engulfed by the cell after four hours of incubation. This was proven by CLSM imaging using *Z*-stacking (Fig. 3). For this experiment, the cells were stained by calcein according to the protocol elaborated earlier.[34] The red satellite (prepared

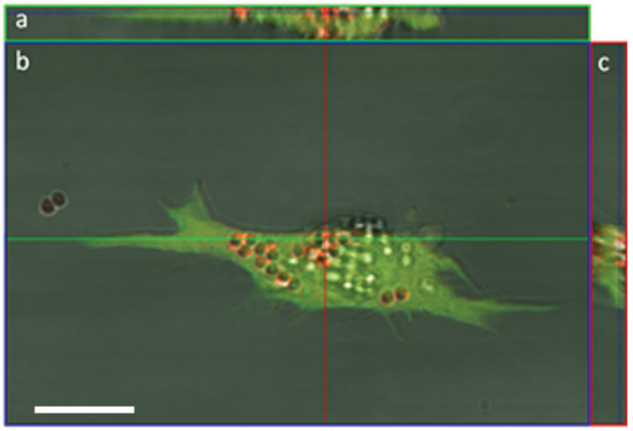

Fig. 3 (b) CLSM image of L929 mouse fibroblast cell after 4 hours of incubation with SiO_2/(PAH-TRITC/Astralen)$_3$/Au particles. The cell has been stained by calcein (green color). (a) and (c) Reconstruction images made from the *Z*-stacking of profiles obtained along the red and green lines on the image (b), respectively. Scale bar equals 20 μm.

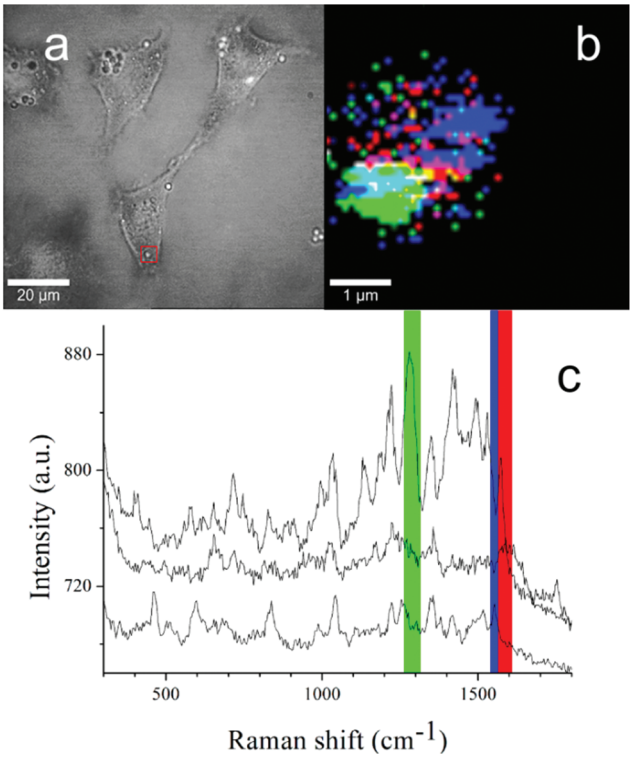

Fig. 4 (a) Optical image of L929 mouse fibroblast cells after 4 hours of incubation with SiO_2/(PAH/Astralen)$_3$/Au satellites; (b) mapping of the Raman signals coming from the area (red rectangle) depicted in the image (a) according to the chosen characteristic bands represented in image (c). The characteristic bands of astralen (in red), DNA (in blue), and lipids (in green) are highlighted in spectra (c). The spectra are taken at a wavelength of 785 nm and a power of 0.2 μW.

using PAH-tetramethylrhodamine (PAH-TRITC)) can be easily recognized in the green-colored cell (Fig. 3b). The *Z*-stacking reconstruction profiles were obtained along two perpendicular lines (red and green), which went through the satellites and the cell. In spite of the fact that the resolution of *Z*-stacking is not high enough compared to *XY*-plane scanning,[35] one can clearly see that the satellites were located next to the bottom of the glass but not on top of the cell. This observation proves that the cells engulfed the satellites after four hours of incubation.

The cytotoxicity analysis was performed by the MTT technique using a mouse fibroblast (cell line L929). The cells were cultivated in Dulbecco's modified Eagle's medium (DMEM) supplemented with 10% FBS in culture flasks (25 cm^2) in a CO_2 incubator at 37 °C in a humidified atmosphere containing 5% of CO_2. To carry out the MTT test, the cells were seeded into 96-well plates (10^4 cells per well) and exposed in a CO_2 incubator, in the presence of various SERS platforms, for 24 hours. As seen in Fig. 1, we did not observe any acute cytotoxicity in the range of SERS concentrations (about 1000–2000 particles per well) that were used in this study. The change in cell viability was not statistically significant compared to the control monolayer culture without SERS platforms (Fig. S2†).

Following the navigation experiments, we focused on probing the intracellular environment with the developed satellite. Before Raman experiments, the cell culture medium was replaced by PBS buffer after cell cultivation for approximately 4 hours on a glass substrate. Furthermore, Raman spectra were acquired from the satellite located inside the cell at a laser power of 0.2 μW and irradiation wavelength of 785 nm. This extremely low power usage of the IR laser ensures non-invasive Raman measurements.[36]

Fig. 4 shows the cells with uptaken satellites (a) including the enlarged image with the mapping of the area around the satellite (b). The Raman spectra (c) were obtained and certain bands (green, red and blue) were chosen for mapping the enlarged cell image according to these bands (Fig. 4b). The signals in the spectra came from biologically relevant compounds as identified by colors according to typical Raman spectra bands (Fig. 4b and c). The red area in Fig. 4c corresponds to astralen[30] (typical C=C band oscillation in the range of 1500–1900 cm^{-1}). Astralen can be used as a marker in complex environments such as biological fluids, living tissues and cells.[32] Lipids are shown in green (Fig. 4c) and corresponds to the characteristic bands of ~1656 cm^{-1}, indicating the presence of C–C stretch vibrations, while the position of a band at 1740 cm^{-1} indicates the presence of carbonyl (C=O) stretching bands. In addition to lipid bands, the probe reveals peaks related to aromatic ring vibrations of nucleic acids, namely, DNA/RNA macromolecules (bands at 1314 cm^{-1}, 1376 cm^{-1} and 1479 cm^{-1}), which were marked in blue (Fig. 4b and c).

The two well-identified spots of blue and green show the distribution of nucleic acids and lipids near the satellite surface (Fig. 4b). One can speculate that the cell nucleolus is located on the right side of the satellite and the lipid membrane, underneath the satellite, on the left. This may happen because the size of the satellite (2 μm) is closed to the thick-

ness of a spread cell, and the cellular compartments are expected to be in direct contact with the uptaken satellite. Thus, the satellites prepared in this study may be used for probing intracellular composition by Raman analysis. We believe that a combination of optical tweezers and Raman spectroscopy may open a way to single cell analysis with high spatial and temporal precision, focusing not only on the intracellular composition, but also on the highly-dynamic extracellular microenvironment. Single cell analysis using LbL assembled films loaded with bioactive molecules gives many options for analysing the extracellular microenvironment.[37,38] Externally controlled delivery from microcarriers embedded into the LbL films[39,40] promises new opportunities for localized non-invasive delivery on demand. For this purpose, the encapsulation of fragile biologically active molecules into externally activated containers such as LbL-assembled microcapsules should be further developed.[41,42] The issues considered above might be of great importance for tissue engineering applications and fundamental studies of cell biology.

Conclusions

SERS-active satellites with a multifunctional shell composed of the Raman active compound astralen and electroless plating either Au or Ag nanoparticles assembled by the LbL technique were externally trapped by optical tweezers and located onto the surface of living L929 mouse fibroblasts with micrometer precision. The satellites coming into contact with the cell surface were internalized by the L929 mouse fibroblasts after 4 hours of incubation. It should be noted that it is possible to use the automatic movement of the laser trap,[43] and thus SERS-sensors, to given coordinates for increasing the accuracy of satellite positioning in space. Astralen, as a Raman tag in the SERS satellite shell, enables one to recognize a probe inside the cell. Probing the internal cellular composition by a SERS satellite identifies characteristic cellular biomolecules such as nucleic acids and lipids.

Experimental section

Materials

Poly(allylamine hydrochloride) (PAH, M_w = ~70 000, Sigma-Aldrich), sodium hydroxide, tetrakis (hydroxymethyl) phosphonium chloride (THPC, Fluka), and potassium carbonate were purchased from Sigma-Aldrich (Germany). Sodium chloride (NaCl) was purchased from Merck. Hydrogen tetrachloroaurate trihydrate ($HAuCl_4 \cdot 3H_2O$) was purchased from Alfa Aesar (UK). Astralen particles were produced by the thermal vaporization of graphite anode by an arc discharge using special conditions of vaporization, extraction and subsequent treatment of the cathode deposit.[30] Graphite powder produced from a pulverized Alpha Aesar graphite rod (99%) was used. After chemical modification, the surface of the astralen particles contained sulfa and hydroxide groups in the ionized state and was negatively charged at neutral pH. Therefore, the astralen nanoparticles were dispersible in water. Zeta potential of the astralen particles was measured to be −11 ± 5 mV. Silica microspheres (diameter 3.5 μm) were purchased from Bangs Laboratories Inc (USA). Deionized water was obtained using a Vodoley water treatment system (NPP Himelektronika, Russia) or Millipore Milli-Q purification system (Millipore Milli-Q, USA).

Fabrication of the SERS satellites

Silica microparticles (1 mg ml^{-1}) were coated with a $(PAH/astralen)_3$ shell by the layer-by-layer (LbL) method using aqueous PAH solutions (1 mg ml^{-1}) and astralen water dispersion (0.1 mg ml^{-1}) according to the protocol described elsewere.[44,45] Next, an additional layer of metal (silver or gold) was deposited on the surface by chemical reduction on the surface of the coated microspheres. The modification of the microsphere surface by silver was carried out in two stages using the well-known silvered mirror reaction. First, 10 μl of silver nitrate solution (0.01 M, reagent grade) and 10 μl of L-ascorbic acid solution (0.1 M, reagent grade) were added to 1 ml of dilute suspension of the LbL-coated microspheres. The mixture was carefully shaken, and then 100 μl of silver nitrate was added. The microsphere suspension became less transparent due to silver coating of the suspended particles. The metal-coated microspheres were washed 5 times with water by centrifugation (6000 rpm, 20 s) followed by re-dispersion. The modification of the microspheres by a gold layer was made using the two-stage protocol previously reported for silica/gold nanoshell synthesis.[46] The "growth" solution was prepared by adding 50 mg of K_2CO_3 to 100 ml of water followed by the addition of 3 ml of 1% $HAuCl_4$ solution. For the preparation of gold seeds, 220 μl of 1 M aqueous NaOH solution and 6 μl of 80% THPC solution were added to 20 ml of water. The obtained solution was vigorously agitated on a magnetic stirrer at 1000 rpm, and then 880 μl of 1% $HAuCl_4$ solution was added. The solution color changed from yellow to brown immediately after adding the $HAuCl_4$ solution, indicating the formation of gold particles (size of about 2 nm). Then, 1 ml of gold nuclei was added to 300 μl of the LbL coated microspheres. The obtained mixture was incubated with shaking for 15 min. After centrifugation, 0.5 ml of water was added to the microsphere suspension. Furthermore, 1 ml of the growth solution and 10 μl of hydrogen peroxide (3.7% water solution) were added to the microspheres decorated with gold nanoparticles (300 μl). The color of the obtained suspension changed from pink to blue-violet. Finally, the obtained particles were washed by centrifugation (6000 rpm 20 s) followed by re-dispersion in water. Core–shell particles were transferred to PBS buffer directly before the cellular experiments.

Characterization

The prepared samples were placed on electrically conductive glass slides covered with ITO (indium-tin oxide), dried and investigated by SEM. The SEM images were recorded by a LEO

1550 Carl Zeiss (Germany) instrument operating at voltage of 3 kV.

Optical tweezers

The optical tweezer setup was equipped with a single-mode continuous-wave diode infrared laser (Lumics LU0975M250, Germany) with a wavelength of 976 nm and output power of up to 250 mW (Fig. S1†). The diode laser was pigtailed by a polarization-maintaining optical fiber, and the output radiation was collimated by an aspheric lens. An oil immersion objective (Olympus UPLFLN 100XOI2, Japan) with numerical aperture of 1.3 and about 60% optical transmittance at 976 nm was used for focusing the laser beam to form the optical trap. To create a maximal optical field gradient at the focal points for the most efficient trapping of micro-objects, the laser beam was expanded to the full objective aperture. The beam shifter, consisting of a system of lenses placed in the confocal configuration, controlled the positioning of the optical trap in the sample area by first moving the lens perpendicular to the beam propagation direction. The extra diode laser with an output power of 0.3 mW at wavelength of 635 nm was used to detect displacements of the trapped micro-objects. The 635 nm beam passed through the optical elements controlling the positions and width of the beam, and was focused into the sample chamber. The forward scattered light was collected by a 40X objective and detected using quadrant photodiodes (QPD) (Thorlabs PDQ80A, USA). Displacements of the trapped objects were extracted from the changes in the QPD photocurrent collected by an analog-to-digital converter (National Instruments PCIe-6353, USA) working at a rate of 105 samples per second per each channel. The CCD camera was used for visual control of the trapped objects. This method is particularly sensitive for measuring the displacements of the trapped spherical objects on the nanometer scale. The hermetic observation chamber was made of a micro-object suspension placed between two coverslips separated by a gap of about 0.15 mm. The observation chamber was placed on a two-coordinate motorized stage for fine sample positioning in the focal plane.

Raman spectroscopy

A Raman confocal microscope (CRM200, WITec, Ulm, Germany) equipped with a piezo-scanner (P-500, Physik Instrumente, Karlsruhe, Germany) and a diode-pumped 785 nm excitation NIR laser (Toptica Photonics AG, Graefelfing, Germany) was used in this study. The laser beam was focused through a 60× water-immersion microscope objective (Nikon, NA = 1.0). The spectra were acquired with a thermoelectrically cooled CCD detector (DU401ABV, Andor, UK) behind a grating (300 g mm^{-1}) spectrograph (Acton, Princeton Instruments Inc., Trenton, NJ, USA) with a spectral resolution of 6 cm^{-1}.

For imaging, an integration time of 0.5 s per pixel was used. The ScanCtrlSpectroscopyPlus software (version 1.38, Witec) and WITec Project Plus (version 2.02, Witec) were used for measurements and for spectral processing, respectively. Calculated single spectra were exported into the OPUS software package (version 6.0).

In vitro cell cultivation

Mouse fibroblasts (L929 cell line) were cultivated in Dulbecco's modified Eagle's medium (DMEM) supplemented with 10% fetal bovine serum (GIbco) in culture flasks (25 cm^2) in a CO_2-incubator under a 5% CO_2 atmosphere at 37 °C. The medium was replaced and the cells were reseeded every 2–4 days.

Acknowledgements

D. V. acknowledges the Alexander von Humboldt Foundation for support (Sofja Kovalevskaja Program). The study was partially supported by RFBR, research project No. 12-03-33088 mol_a_ved and research project No. 14-02-31089 mol_a, the grants of the Russian Scientific Foundation (project no. 14-13-01167), Government of the Russian Federation (grant №14.Z50.31.0004), DAAD A/12/86694. The authors thank Rona Pitschke for SEM measurements. We are also grateful to Roman Schuetz for help with Raman experiments and Thomas Paulraj for help with cell staining and imaging. We want to acknowledge Andrey N. Ponomarev, Head of Science & Technical Center of Applied Researches (St-Petersburg, Russia) for providing the astralen nanoparticles for this study.

Notes and references

1 D. Wang and S. Bodovitz, *Trends Biotechnol.*, 2010, **28**, 281–290.
2 F. S. O. Fritzsch, C. Dusny, O. Frick and A. Schmid, in *Annual Review of Chemical and Biomolecular Engineering*, ed. J. M. Prausnitz, 2012, vol. 3, pp. 129–155.
3 T. Graf and M. Stadtfeld, *Cell Stem Cell*, 2008, **3**, 480–483.
4 K. Kleparnik and F. Foret, *Anal. Chim. Acta*, 2013, **800**, 12–21.
5 T. C. Chao and A. Ros, *J. R. Soc. Interface*, 2008, **5**, S139–S150.
6 M. Harz, M. Kiehntopf, S. Stockel, P. Rosch, T. Deufel and J. Popp, *Analyst*, 2008, **133**, 1416–1423.
7 C. Krafft, B. Dietzek and J. Popp, *Analyst*, 2009, **134**, 1046–1057.
8 K. Kneipp, Y. Wang, H. Kneipp, L. T. Perelman, I. Itzkan, R. R. Dasari and M. S. Feld, *Phys. Rev. Lett.*, 1997, **78**, 1667–1670.
9 R. J. Swain and M. M. Stevens, *Biochem. Soc. Trans.*, 2007, **35**, 544–549.
10 W. Xie, C. Herrmann, K. Kömpe, M. Haase and S. Schlücker, *J. Am. Chem. Soc.*, 2011, **133**, 19302–19305.
11 C. Leordean, M. Potara, S. Boca-Farcau, A. Vulpoi, S. Astilean and C. Farcau, *J. Raman Spectrosc.*, 2014, **45**, 627–635.
12 U. Huebner, H. Schneidewind, D. Cialla, K. Weber, M. Zeisberger, R. Mattheis, R. Moeller and J. Popp, Fabrica-

tion of regular patterned SERS arrays by electron beam lithography, in *Biophotonics: Photonic Solutions for Better Health Care II*, ed. J. Popp, V. V. Tuchin and D. L. Matthews, 2010, vol. 7715.
13 W.-D. Li, J. Hu and S. Y. Chou, *Opt. Express*, 2011, **19**, 21098–21108.
14 L. Zhong, X. Zhou, S. Bao, Y. Shi, Y. Wang, S. Hong, Y. Huang, X. Wang, Z. Xie and Q. Zhang, *J. Mater. Chem.*, 2011, **21**, 14448–14455.
15 R. A. Alvarez-Puebla, A. Agarwal, P. Manna, B. P. Khanal, P. Aldeanueva-Potel, E. Carbó-Argibay, N. Pazos-Pérez, L. Vigderman, E. R. Zubarev, N. A. Kotov and L. M. Liz-Marzán, *Proc. Natl. Acad. Sci. U. S. A.*, 2011, **108**, 8157–8161.
16 A. Guerrero-Martínez, S. Barbosa, I. Pastoriza-Santos and L. M. Liz-Marzán, *Curr. Opin. Colloid Interface Sci.*, 2011, **16**, 118–127.
17 L. Rodríguez-Lorenzo, R. de la Rica, R. A. Álvarez-Puebla, L. M. Liz-Marzán and M. M. Stevens, *Nat. Mater.*, 2012, **11**, 604–607.
18 P. Sajanlal and T. Pradeep, *Nano Res.*, 2009, **2**, 306–320.
19 Z. Huang, G. Meng, Q. Huang, B. Chen, C. Zhu and Z. Zhang, *J. Raman Spectrosc.*, 2013, **44**, 240–246.
20 I. Yoon, T. Kang, W. Choi, J. Kim, Y. Yoo, S.-W. Joo, Q. H. Park, H. Ihee and B. Kim, *J. Am. Chem. Soc.*, 2008, **131**, 758–762.
21 G. Rusciano, A. C. De Luca, A. Sasso and G. Pesce, *Anal. Chem.*, 2007, **79**, 3708–3715.
22 M. J. Guffey and N. F. Scherer, *Nano Lett.*, 2010, **10**, 4302–4308.
23 G. McNay, F. T. Docherty, D. Graham, W. E. Smith, P. Jordan, M. Padgett, J. Leach, G. Sinclair, P. B. Monaghan and J. M. Cooper, *Angew. Chem., Int. Ed.*, 2004, **43**, 2512–2514.
24 C. Jiang, S. Markutsya, Y. Pikus and V. V. Tsukruk, *Nat. Mater.*, 2004, **3**, 721–728.
25 C. Lu, H. Möhwald and A. Fery, *J. Phys. Chem. C*, 2007, **111**, 10082–10087.
26 A. Yashchenok, A. Masic, D. Gorin, B. S. Shim, N. A. Kotov, P. Fratzl, H. Möhwald and A. Skirtach, *Small*, 2013, **9**, 351–356.
27 C. S. Peyratout and L. Dahne, *Angew. Chem., Int. Ed.*, 2004, **43**, 3762–3783.
28 A. L. Becker, A. P. R. Johnston and F. Caruso, *Small*, 2010, **6**, 1836–1852.
29 S. A. Sukhishvili, *Curr. Opin. Colloid Interface Sci.*, 2005, **10**, 37–44.
30 A. I. Shames, E. A. Katz, A. M. Panich, D. Mogilyansky, E. Mogilko, J. Grinblat, V. P. Belousov, I. M. Belousova and A. N. Ponomarev, *Diamond Relat. Mater.*, 2009, **18**, 505–510.
31 R. Stiufiuc, C. Iacovita, C. Lucaciu, G. Stiufiuc, A. Dutu, C. Braescu and N. Leopold, *Nanoscale Res. Lett.*, 2013, **8**, 47.
32 I. Y. Stetciura, A. V. Markin, A. N. Ponomarev, A. V. Yakimansky, T. S. Demina, C. Grandfils, D. V. Volodkin and D. A. Gorin, *Langmuir*, 2013, **29**, 4140–4147.
33 A. Gutés, R. Maboudian and C. Carraro, *Langmuir*, 2012, **28**, 17846–17850.
34 T. Paulraj, N. Feoktistova, N. Velk, C. Duschl and D. Volodkin, *Macromol. Rapid Commun.*, 2014, **35**(16), 1408–1413.
35 K. Uhlig, N. Madaboosi, S. Schmidt, M. S. Jager, J. Rose, C. Duschl and D. V. Volodkin, *Soft Matter*, 2012, **8**, 11786–11789.
36 R. Weissleder, *Nat. Biotechnol.*, 2001, **19**, 316–317.
37 D. Volodkin, R. von Klitzing and H. Moehwald, Polyelectrolyte multilayers: towards single cell studies, *Polymers*, 2014, **6**(5), 1502–1527.
38 D. Volodkin, A. Skirtach and H. Möhwald, *LbL Films as Reservoirs for Bioactive Molecules Bioactive Surfaces*, ed. H. G. Börner and J.-F. Lutz, Springer, Berlin/Heidelberg, 2011, vol. 240, pp. 135–161.
39 D. Volodkin, A. Skirtach and H. Möhwald, Bioapplications of light-sensitive polymer films and capsules assembled using the layer-by-layer technique, *Polym. Int.*, 2012, **61**(5), 673–679.
40 A. G. Skirtach, D. V. Volodkin and H. Mohwald, Bio-interfaces-Interaction of PLL/HA Thick Films with Nanoparticles and Microcapsules, *ChemPhysChem*, 2010, **11**(4), 822–829.
41 D. Volodkin, CaCO3 templated micro-beads and -capsules for bioapplications, *Adv. Colloid Interface Sci.*, 2014, **206**, 437–454.
42 S. Schmidt and D. Volodkin, Microparticulate biomolecules by mild CaCO3 templating, *J. Mater. Chem. B*, 2013, **1**(9), 1210–1218.
43 H. Chen, C. Wang and Y. Lou, *IEEE Trans. Biomed. Eng.*, 2013, **60**, 1518–1527.
44 R. K. Iler, *J. Colloid Interface Sci.*, 1966, **21**, 569–594.
45 G. Decher, J. D. Hong and J. Schmitt, *Thin Solid Films*, 1992, **210–211**(Part 2), 831–835.
46 B. E. Brinson, J. B. Lassiter, C. S. Levin, R. Bardhan, N. Mirin and N. J. Halas, *Langmuir*, 2008, **24**, 14166–14171.

